The Astronomical Journal, 143:25 (8pp), 2012 January doi:10.1088/0004-6256/143/1/25

BINARY ASTEROID ENCOUNTERS WITH TERRESTRIAL PLANETS: TIMESCALES AND EFFECTS

Julia Fang[1] and Jean-Luc Margot[1,2]
[1] Department of Physics and Astronomy, University of California, Los Angeles, CA 90095, USA
[2] Department of Earth and Space Sciences, University of California, Los Angeles, CA 90095, USA
Received 2011 August 3; accepted 2011 November 10; published 2011 December 13

ABSTRACT

Many asteroids that make close encounters with terrestrial planets are in a binary configuration. Here, we calculate the relevant encounter timescales and investigate the effects of encounters on a binary's mutual orbit. We use a combination of analytical and numerical approaches with a wide range of initial conditions. Our test cases include generic binaries with close, moderate, and wide separations, as well as seven well-characterized near-Earth binaries. We find that close approaches (<10 Earth radii) occur for almost all binaries on 1–10 million year timescales. At such distances, our results suggest substantial modifications to a binary's semimajor axis, eccentricity, and inclination, which we quantify. Encounters within 30 Earth radii typically occur on sub-million year timescales and significantly affect the wider binaries. Important processes in the lives of near-Earth binaries, such as tidal and radiative evolution, can be altered or stopped by planetary encounters.

Key words: minor planets, asteroids: general – minor planets, asteroids: individual (2000 DP107, 1999 KW4, 2002 CE26, 2004 DC, 2003 YT1, Didymos, 1991 VH)

Online-only material: color figure

1. INTRODUCTION

Near-Earth asteroids (NEAs) live in a dynamic environment that includes gravitational encounters with planets and the Sun as well as other non-gravitational perturbations, with average dynamical lifetimes on the order of a few million years (Bottke et al. 2002). They are replenished from source regions in the main belt of asteroids, which include strong resonances with Jupiter and Saturn. Radar and light curve studies by Margot et al. (2002) and Pravec et al. (2006) have determined that approximately 15% of these short-lived objects larger than 200 m in diameter are in a binary configuration, with a primary and a secondary orbiting their common center of mass. The mutual orbits of these binary asteroids are affected by tides, by external perturbations such as the radiative binary YORP (BYORP) effect (Ćuk & Burns 2005; Ćuk 2007), and by close encounters with terrestrial planets. In this work, we investigate the effect of close planetary encounters on the mutual binary orbits of NEA systems by studying changes in the semimajor axis, eccentricity, and inclination. We also calculate the frequency of such terrestrial planet flybys.

Early work on the subject of planetary encounters with NEA binaries was accomplished by Farinella (1992) and Farinella & Chauvineau (1993). They employed analytical estimates and Monte Carlo techniques to estimate the change in orbital energy and angular momentum due to an encounter. Recent work by Fang et al. (2011) examined the effect of close planetary encounters on the mutual orbits of NEA triples 2001 SN263 and 1994 CC. They found that scattering events by terrestrial planets can excite the eccentricities as well as mutual inclinations of the satellites' orbits to currently observed values on million-year timescales. During close approaches to Earth, the outer satellites in both triple systems can have their orbital eccentricities excited to values of at least 0.2 as far away as encounter distances of ∼40 Earth radii for 2001 SN263 and ∼50 Earth radii for 1994 CC. Since the orbital effects of encounters on triples have been previously examined, this present study focuses only on binary systems. Other recent studies have invoked planetary encounters to explain the rotational dynamics of asteroids (Scheeres et al. 2004; Sharma et al. 2006), the tidal disruption of rubble pile asteroids to form binaries (Walsh & Richardson 2006), and the re-surfacing of NEAs (Nesvorný et al. 2010; Binzel et al. 2010). Prior studies include Bottke & Melosh (1996a, 1996b), Asphaug & Benz (1996), and Richardson et al. (1998).

In this work, we perform *N*-body simulations and employ analytical expressions to evaluate a binary's orbital changes due to a close planetary encounter with Earth. Initial conditions include three generic cases (a close binary with a separation of 4 primary radii, a moderately separated binary with a separation of 8 primary radii, and a wide binary with a separation of 16 primary radii) as well as parameters drawn from known, well-characterized NEA binaries. By "well-characterized" we mean a binary for which the system mass, semimajor axis, eccentricity, and approximate component sizes are known—in practice this corresponds to a subset of the radar-observed binaries. Table 1 shows a compilation of these binaries and their parameters such as primary size, primary mass, and primary–secondary separation. In Section 2, we perform single flyby simulations and use analytical equations to determine the orbital effects of a close planetary encounter, by thoroughly examining a variety of encounter geometries, distances, and velocities. We study the changes in the semimajor axis, eccentricity, and inclination of the binary orbit. In Section 3, we present long-term simulations with test particles and planets to calculate encounter timescales for observed NEA binaries whose encounter frequencies are strongly dependent on their individual evolutionary histories. We discuss and summarize this study in Section 4.

2. EFFECT OF A SINGLE PLANETARY ENCOUNTER

2.1. Methods

We perform *N*-body numerical integrations to investigate the effects of a close approach to an Earth-mass planet on a binary's mutual orbit. We use a Bulirsch–Stoer algorithm from an *N*-body numerical integration package, *Mercury* (Chambers

Table 1
Well-characterized Near-Earth Binaries

System	R_p (km)	M_p (kg)	a (km)	a/R_p	$a_\odot$ (AU)	$e_\odot$	$i_\odot$ (deg)
(185851) 2000 DP107[a]	0.40	4.38×10^{11}	2.62	6.6	1.37	0.38	8.67
(66391) 1999 KW4[b]	0.66	2.35×10^{12}	2.55	3.9	0.64	0.69	38.89
(276049) 2002 CE26[c]	1.75	2.17×10^{13}	4.87	2.8	2.23	0.56	47.31
2004 DC[d]	0.17	3.57×10^{10}	0.75	4.4	1.63	0.40	19.45
(164121) 2003 YT1[e]	0.55	1.89×10^{12}	3.93	7.1	1.11	0.29	44.06
(65803) Didymos[f]	0.40	5.24×10^{11}	1.18	3.0	1.64	0.38	3.41
(35107) 1991 VH[g]	0.60	1.40×10^{12}	3.26	5.4	1.14	0.14	13.91

Notes. Well-characterized near-Earth binaries and their parameters are compiled in this table, including the radius of the primary R_p, mass of the primary M_p, semimajor axis a (in units of km), and semimajor axis divided by the primary radius a/R_p. Rough uncertainties in binary parameters are ~20% in sizes, ~10% in masses, and $\lesssim$5%–10% in semimajor axes. Heliocentric orbital data are given for the semimajor axis $a_\odot$, eccentricity $e_\odot$, and inclination $i_\odot$ with respect to the ecliptic.

[a] Margot et al. (2002) and Naidu et al. (2011).
[b] Ostro et al. (2006).
[c] Shepard et al. (2006).
[d] Taylor et al. (2008).
[e] Nolan et al. (2004).
[f] Benner et al. (2010).
[g] Margot et al. (2008) and Pravec et al. (2006).

1999). Our simulations incorporate three massive bodies (all assumed to be spherical), which include an asteroid binary and an Earth-mass perturber on a hyperbolic trajectory at various close encounter distances. We explore a wide range of initial conditions in encounter distance and velocity, which we describe in detail below. For each pair of encounter distance and velocity, systematic simulations are performed with nearly 7000 permutations of the following mutual orbital parameters: inclination, longitude of the ascending node, and mean anomaly. Our test cases include all of the NEA binaries shown in Table 1 as well as a few generic cases with a typical rubble pile density of 2 g cm^{-3} and a primary radius of 0.5 km: a close binary with a separation of 4 primary radii, a moderately separated binary with a separation of 8 primary radii, and a wide binary with a separation of 16 primary radii.

The hyperbolic encounter velocity v_∞, defined as the relative speed between the binary and Earth at infinity, can be described by a probability distribution of relative velocities as shown in Figure 1. As a result, our simulations appropriately cover a range of v_∞ from 8 to 24 km s^{-1} with increments of 4 km s^{-1}. We also systematically repeat the ensemble of simulations for various close encounter distances whose range is dependent on the binary's semimajor axis and with typical increments of 1–2 $R_\oplus$.

In this paper, the "encounter distance" q is defined as the distance of closest approach and the "impact parameter" b is the hypothetical encounter distance that would result in the absence of gravitational focusing. The impact parameter can be described as the perpendicular distance between the non-focused path of the perturber and the binary. The usual definition relating impact parameter b and encounter distance q is $b^2 = q^2(1 + (2GM_\oplus)/(q v_\infty^2))$, where G is the gravitational constant, $M_\oplus$ is the mass of the Earth, and v_∞ is the encounter velocity at infinity. For most cases we consider here, the difference between b and q is less than 1 Earth radius.

All of the simulations begin with asteroid binaries in circular orbits. After a scattering encounter, possible outcomes include (1) an intact, stable binary system, or instability marked by (2) collision between any two bodies or (3) ejection of the secondary from the binary system. Encounter results are recorded for

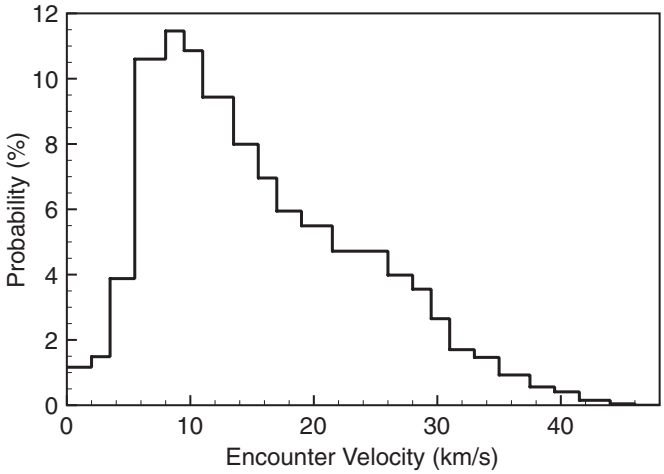

Figure 1. Probability distribution of expected encounter velocities v_∞ of NEAs with Earth is obtained from numerical simulations of asteroid migration from source regions (Mars-crossing region, ν_6 resonance, and 3:1 mean-motion resonance with Jupiter) in or adjacent to the main belt (B. Bottke & K. Walsh 2011, private communication).

changes in the semimajor axis, eccentricity, and inclination in stable encounters only. Stable systems are defined as binaries with no collisions nor ejections of the secondary.

The output from numerical simulations is compared with approximate analytical results. We consider close planetary encounters with NEA binaries to be impulsive events, defined as swift encounters where the planet's interaction with the binary is much shorter than the orbital period of the binary. The encounter delivers an impulse representing a shift in velocity of the binary's orbit, and this impulse approximation is valid in the domain where $q/v_\infty \ll P$, where P is the binary's mutual orbital period. For such impulsive encounters, the change in a binary's orbital elements has been analytically approximated by previous studies. Heggie & Rasio (1996) derived the change in a binary's eccentricity, Collins & Sari (2008) derived the change in both eccentricity and inclination, and Farinella & Chauvineau (1993) and Chauvineau & Farinella (1995) derived the change in energy (which we can relate to a change in the semimajor

axis). The typical change in a binary's orbital elements after averaging over all encounter geometries (which include stable and unstable encounters) can be estimated as

$$\Delta a \approx 1.48\sqrt{\frac{G}{M}}\frac{M_\oplus a^{5/2}}{v_\infty q^2} \quad (1)$$

$$\Delta e \approx 1.89\sqrt{\frac{G}{M}}\frac{M_\oplus a^{3/2}}{v_\infty q^2} \quad (2)$$

$$\Delta i \approx 0.75\sqrt{\frac{G}{M}}\frac{M_\oplus a^{3/2}}{v_\infty q^2}, \quad (3)$$

where G is the gravitational constant, $M_\oplus$ is the mass of the Earth, v_∞ is the encounter velocity, and q is the encounter distance. The binary's semimajor axis is represented by a, its eccentricity is e, its inclination is i, and its system mass is M. The constants in front of Equations (2) and (3) represent the averaging of encounter geometries and have been calculated by Collins & Sari (2008). In their paper, we note there is a factor of two missing in the denominator of Equation (A3). By analogy, we obtain the constant in front of Equation (1) by scaling the analytical curve to our numerical simulation results.

2.2. Results

The change in the semimajor axis due to a planetary flyby is shown for three generic cases presented in Figure 2. Output from numerical simulations is shown as points and represents the mean values of the change (after taking the absolute value) in the semimajor axis resulting from stable encounters. The curves represent analytical estimates, which provide a reasonable match to our numerical results. We show the average changes in the semimajor axis for $v_\infty = 12$, 16, 20, and 24 km s^{-1}. The results using a v_∞ of 8 km s^{-1} are not shown because the resulting spread in the post-encounter semimajor axis is very broad (e.g., at an encounter distance of 10 Earth radii, the standard deviation is ~2.1 km) and not accurately portrayed by a single value. We wish to show orbital effects of only stable encounters; the range of close encounter distances for each binary type shown in this figure is determined by the distances at which all encounters resulted in stable binaries. Since the three types of binaries have different separations, they will have different ranges of encounter distances at which stable encounters occur. These plots show that larger binary separations produce greater changes in the semimajor axis at any given encounter distance because wider binaries are less tightly bound and thus more susceptible to passing perturbers.

The change in eccentricity is shown in Figure 3, with similar encounter distance and velocity ranges as shown in Figure 2. Results from numerical simulations are given as the mean value of the eccentricity increase of all stable encounters. Analytical and numerical results are in agreement, especially for greater encounter velocities. For our test NEA binaries (Table 1) and using a typical v_∞ of 12 km s^{-1}, we also show the close encounter distances at which their eccentricities can be excited to a value of at least 0.2 (Figure 4) and how the distance at which eccentricity excitation occurs is a function of binary separation (Figure 5). The eccentricity excitation distance is defined in Figure 5 as the encounter distance where 50% of stable encounters resulted in binaries with $e \geqslant 0.2$. Since it is evident from this figure that there is a relationship between the critical encounter distance q and the binary's semimajor axis

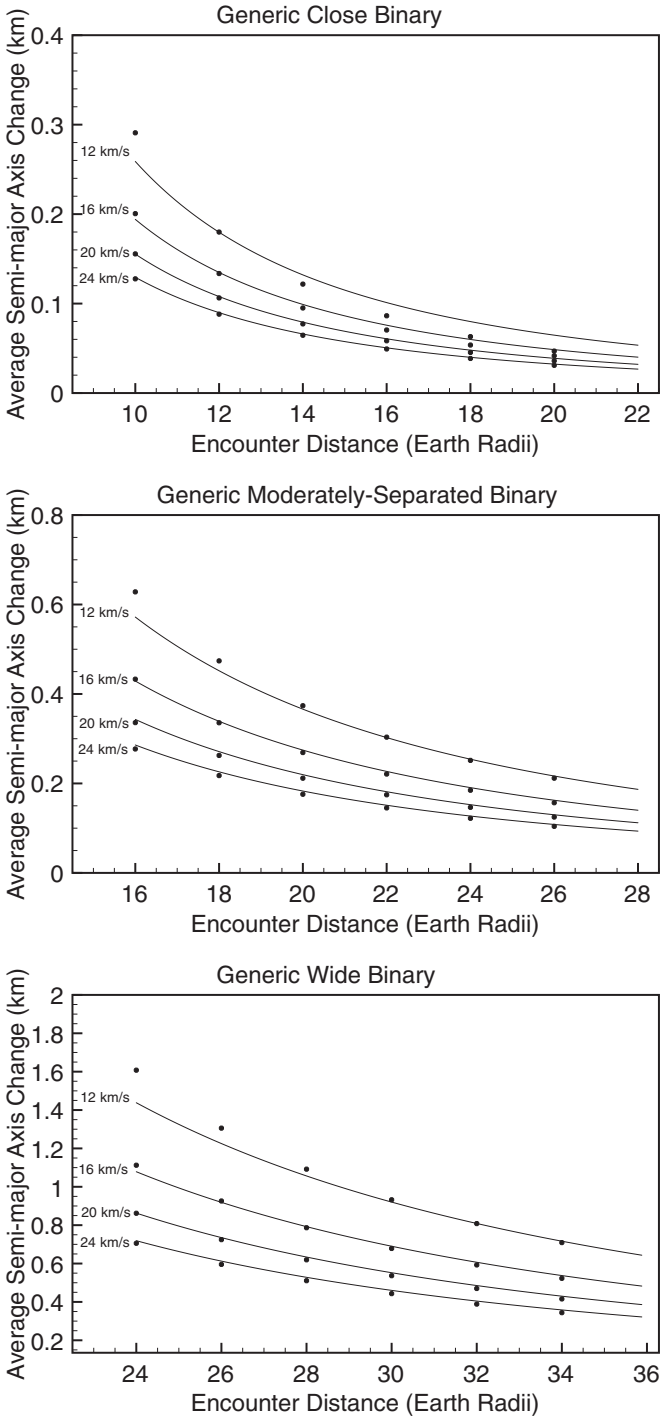

Figure 2. Change in a binary's semimajor axis is shown as a function of encounter distance and velocity for three types of binaries: close binaries, moderately separated binaries, and wide binaries. Results from numerical simulations are shown as dots and analytical calculations are depicted by solid lines.

a (when expressed in units of primary radii), we solve for its analytical relationship by rearranging Equation (2) and find

$$\frac{q}{R_\oplus} \approx \frac{1}{R_\oplus}\left(\frac{1.89\,M_\oplus}{\Delta e\, v_\infty}\right)^{1/2}\left(\frac{3G}{4\pi\rho}\right)^{1/4}\left(\frac{a}{R_p}\right)^{3/4}, \quad (4)$$

where R_p is the primary's mass, $R_\oplus$ and $M_\oplus$ are the radius and mass of the Earth, G is the gravitational constant, Δe is the

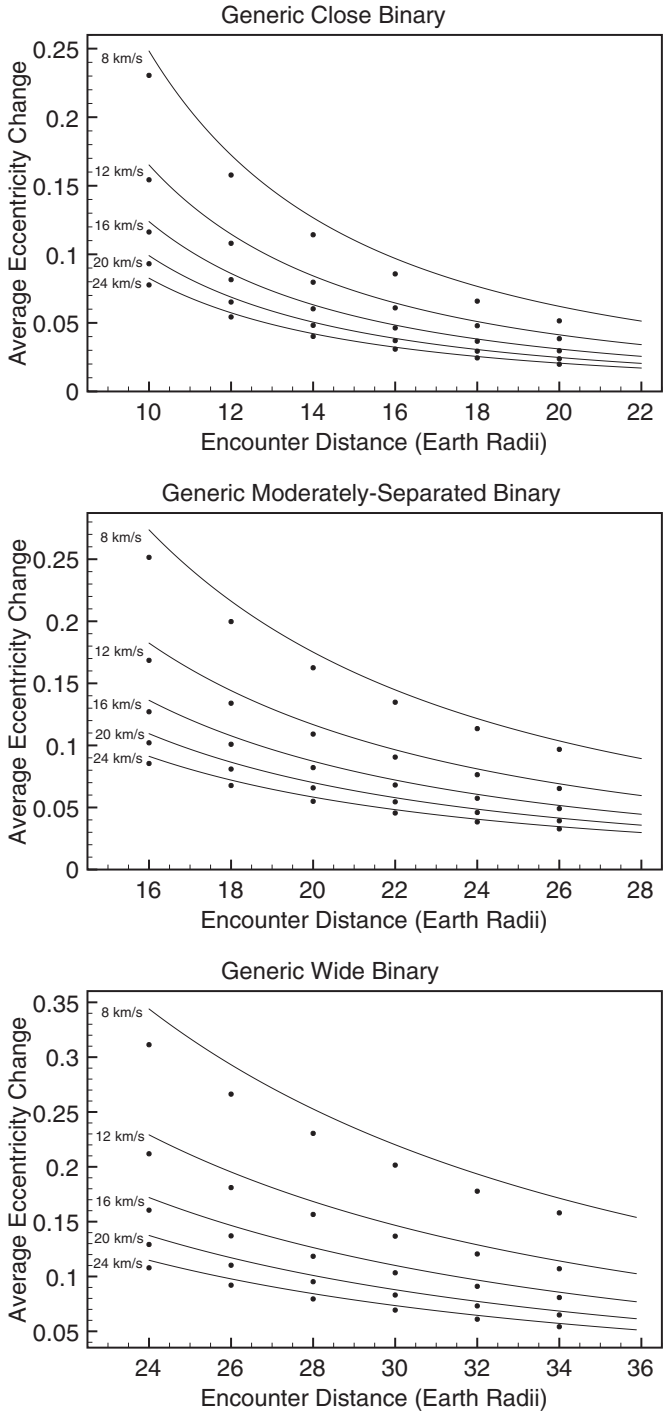

Figure 3. Change in a binary's eccentricity is shown as a function of encounter distance and velocity for three types of binaries: close binaries, moderately separated binaries, and wide binaries. Results from numerical simulations are shown as dots and analytical calculations are depicted by solid lines.

change in eccentricity due to the encounter, v_∞ is the encounter velocity, and ρ is the binary's density.

As stated earlier, the 1.89 factor is due to averaging over all angles of encounter geometries (Collins & Sari 2008). This equation is valid for initially circular binaries. The same $q \propto a^{3/4}$ relationship holds for all binaries in our sample because for a uniform set of encounter parameters (encounter velocity and perturber's radius and mass), encounter strength (strong enough to excite $\Delta e = 0.2$), and binary density (assuming NEA

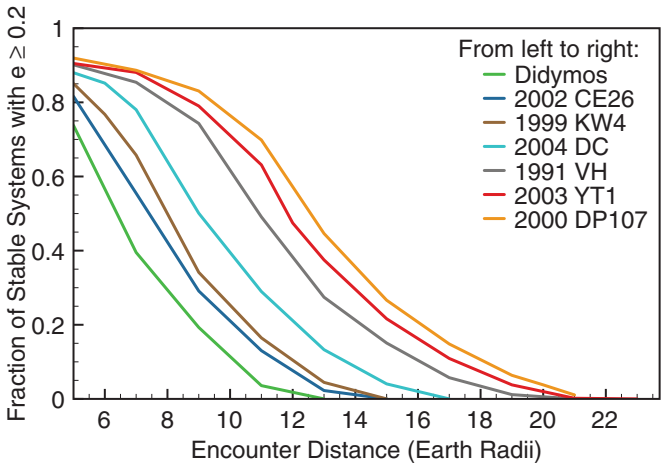

Figure 4. Using orbital and physical parameters from the sample of NEA binaries given in Table 1, we show the fraction of stable systems (no ejections nor collisions) with excited eccentricities ($e \geqslant 0.2$) as a function of encounter distance for $v_\infty = 12$ km s^{-1}.

(A color version of this figure is available in the online journal.)

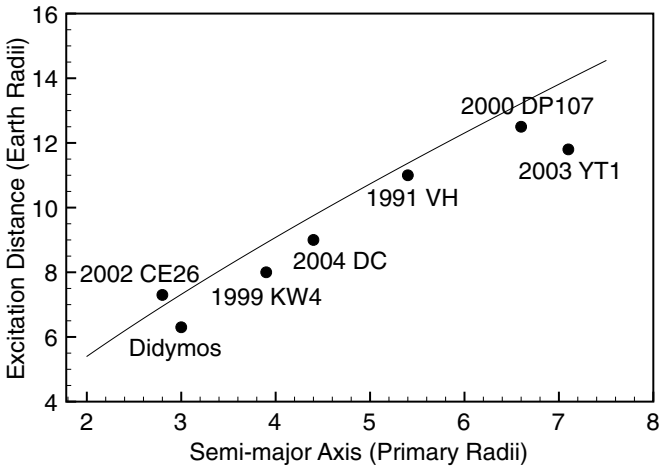

Figure 5. Eccentricity excitation distance (defined as the close encounter distance where 50% of stable NEA binary systems showed $e \geqslant 0.2$) is given as a function of the secondary's semimajor axis in units of primary radii. The curve shows the result obtained from the analytical expression. This case is for v_∞ of 12 km s^{-1}.

binaries have similar rubble pile densities), the prefactor in front of the $a^{3/4}$ term is constant. In convenient units,

$$\frac{q}{R_\oplus} \approx 3.21 \left(\frac{0.2}{\Delta e} \times \frac{12\,\mathrm{km\,s^{-1}}}{v_\infty}\right)^{1/2} \left(\frac{2\,\mathrm{g\,cm^{-3}}}{\rho}\right)^{1/4} \left(\frac{a}{R_p}\right)^{3/4}. \quad (5)$$

We overplot this analytical relationship in Figure 5 and find a good match to the numerical results. The agreement between numerical and analytical estimates for 2003 YT1 is not as good due to its higher density estimate (its nominal density is $\rho \sim 2.7$ g cm^{-3}), since we assumed $\rho = 2$ g cm^{-3} in the calculation of Equation (5).

In Figure 6, we show the eccentricity excitation behavior due to $v_\infty = 8$, 12, 16, 20, and 24 km s^{-1} for specific observed NEA binaries: a close binary (depicted by 1999 KW4), a moderately separated binary (2000 DP107), and a wide binary (represented by a hypothetical binary with a 16 primary radii separation). As the value of v_∞ decreases, a greater fraction of stable systems have excited eccentricities due to a planetary flyby at a given encounter distance. In addition, as the value of v_∞ decreases,

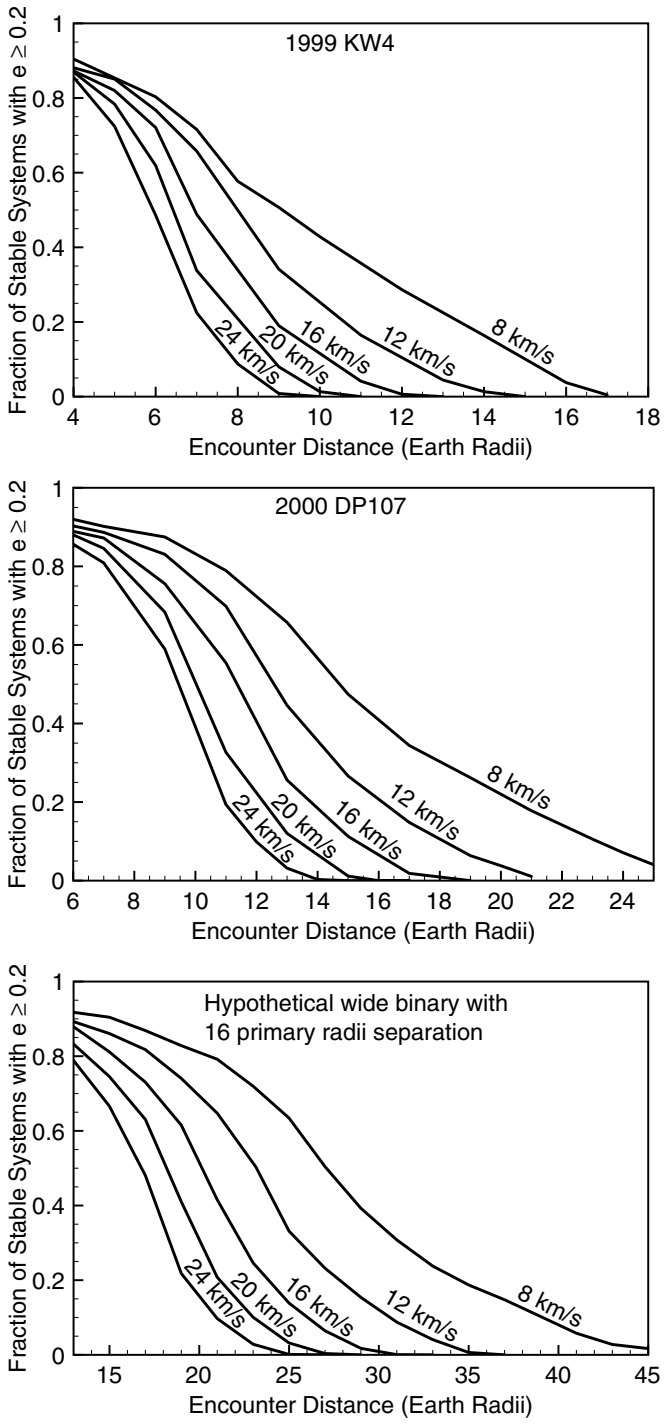

Figure 6. Characteristic behavior of close NEA binaries (i.e., 1999 KW4), moderately separated NEA binaries (i.e., 2000 DP107), and wide NEA binaries (represented by a hypothetical binary with a separation of 16 primary radii) due to varying encounter velocities (v_∞ = 8–24 km s^{-1} with increments of 4 km s^{-1}) is shown. The fraction of stable systems (no ejections nor collisions) with excited eccentricities ($e \geqslant 0.2$) is shown as a function of encounter distance.

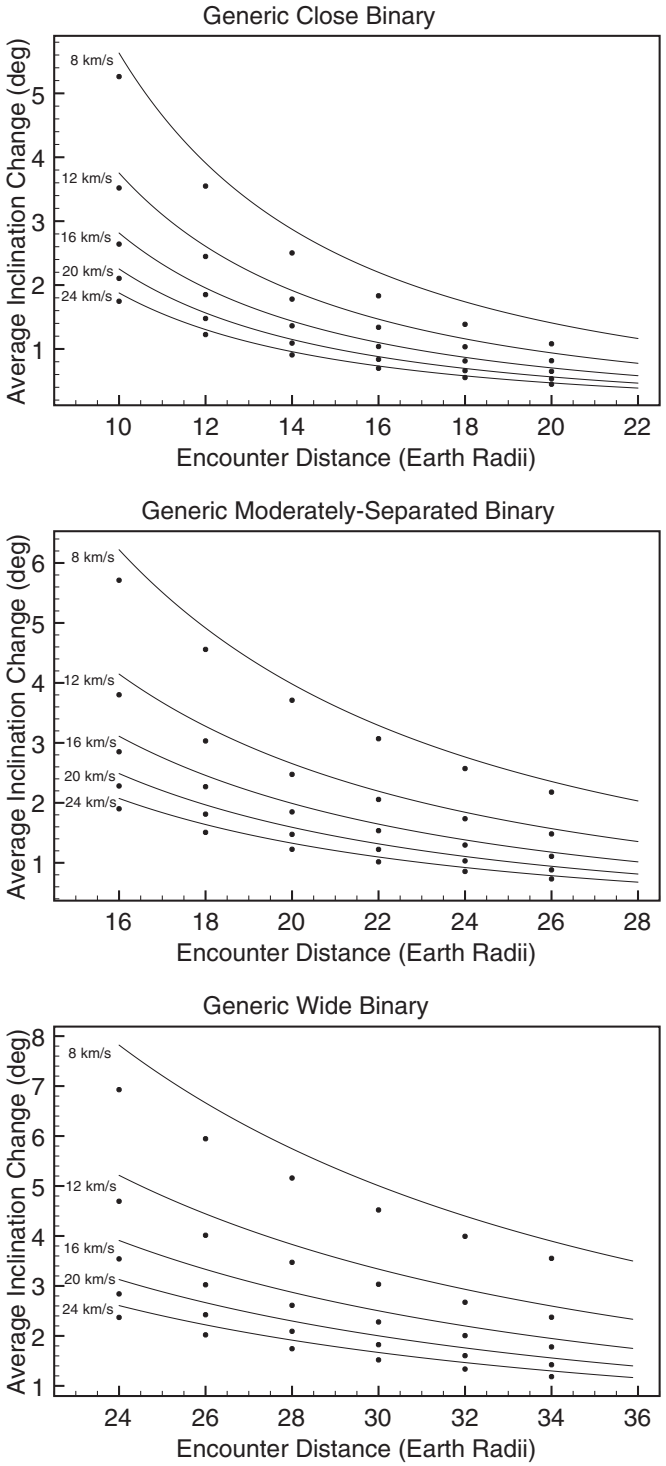

Figure 7. Change in a binary's inclination is shown as a function of encounter distance and velocity for three types of binaries: close binaries, moderately separated binaries, and wide binaries. Results from numerical simulations are shown as dots and analytical calculations are depicted by solid lines.

the final eccentricities of binaries in our simulations increased. These effects occur because a slower-passing perturber will have a longer encounter duration with the binary and therefore cause a stronger perturbation on the binary's mutual orbit.

The change in a binary's orbital inclination is shown in Figure 7, with similar encounter distances and velocities as shown in Figures 2 and 3. Results from numerical simulations are given as the mean value of the inclination change of all stable encounters. Comparison between output from numerical simulations and analytical estimates provide a decent match. Possible reasons for the less-than-exact agreement between numerical and analytical results include our choice of using the mean value to represent the average change in inclination of stable encounters from simulations as well as the practical limit on the number of encounter geometries we were able to perform in our simulations. The analytical expressions are also

only valid in the limit of impulsive encounters, suggesting that analytical results should provide better matches to simulations with faster encounter velocities, which is consistent with our results.

These results have implications for binaries observed with excited dynamical states. For instance, previous studies of 1999 KW4 (heliocentric a is 0.64 AU, e is 0.69, i is 38.°89; current solar close approach distance is 0.2 AU) suggest that the binary's close approaches to the Sun can excite its rotational and orbital states (Ostro et al. 2006; Scheeres et al. 2006). Their numerical simulations show that the binary's mutual orbit pole can be modified by more than 0.°5 per pericenter passage for a pericenter distance of 0.2 AU and by more than 1° for a pericenter distance of 0.12 AU. From our simulations, we find that planetary encounters with an Earth-mass body can perturb the binary orbit pole by a similar amount. Therefore, even NEAs that do not come as close to the Sun as 1999 KW4 may exhibit excited rotational and orbital dynamics. For a generic binary with a semimajor axis of four primary radii (same as 1999 KW4's separation), our simulations using v_∞ from 8 to 24 km s^{-1} show that a 0.°5 shift in inclination can occur due to a planetary encounter at distances of 18–28 $R_\oplus$ and a 1° shift can occur at 13–20 $R_\oplus$.

We briefly discuss instability trends seen in simulations with a typical v_∞ of 12 km s^{-1} for observed NEA binaries (Table 1). For nearly all encounter distances sampled in simulations, ejections dominated over collisions in unstable encounters. If planetary encounters close enough to disrupt a binary have occurred, an ejected secondary is more likely to occur than a collision between the primary and secondary. Therefore one would expect that planetary encounters can lead to the formation of asteroid pairs in the near-Earth population, in addition to the formation mechanisms responsible for pair production in the main belt. The different routes toward the creation of asteroid pairs are discussed in a companion paper by Fang & Margot (2012). Close binaries such as Didymos, 2002 CE26, 1999 KW4, and 2004 DC have similarly small component separations (2–5 R_p) relative to their primary's radius R_p and exhibit comparable disruption statistics. Instabilities, including both ejections and collisions, occurred at encounter distances of ∼5–7 $R_\oplus$ and less. More moderately spaced binaries such as 2000 DP107, 2003 YT1, and 1991 VH have comparable component separations (5–9 R_p). For these binaries, simulation results showed disruption occurring at encounter distances of ∼7–9 $R_\oplus$ and less. Binaries with wide separations will have mutual orbits that are more easily perturbed than tighter systems.

Given the significant orbital perturbations in binary systems that can be caused by planetary flybys, the next section examines the frequency of such encounters.

3. FREQUENCY OF PLANETARY ENCOUNTERS

3.1. Methods

After investigating the orbital effects of a single planetary flyby on a binary in Section 2, we next determine the frequency of such close planetary encounters with Earth for well-characterized NEA binaries (Table 1). The timescale of close encounters is very dependent on the specific NEA's past evolutionary path to its current heliocentric orbit (see Table 1 for current heliocentric parameters), and different NEAs can have very different close encounter histories. We do not backward-integrate the current heliocentric orbits because the orbits become chaotic over time and it is difficult to reconstruct their past history, even statistically. Consequently, we follow the methods of Bottke et al. (2002) by integrating test particles from the three strongest source regions (ν_6 secular resonance with Saturn, 3:1 mean-motion resonance with Jupiter, and Mars-crossing regions) in or adjacent to the main belt and by tracking the test particles as they migrate into near-Earth space. These source regions are the main dynamical pathways to NEA orbits. Integrations are performed using a hybrid symplectic/Bulirsch–Stoer algorithm from *Mercury* (Chambers 1999) and include the Sun and all eight planets in addition to 3000 test particles per source (9000 test particles total). In the simulations, we ignore the effect of Yarkovsky. The Yarkovsky effect is an important perturbation that moves asteroids into main-source regions; however, once asteroids have reached the source regions, the effect of Yarkovsky is negligible compared to the effect of strong resonances and planetary encounters.

After test particles have migrated into near-Earth space, we search for particles whose orbital elements (semimajor axis a, eccentricity e, and inclination i) closely match the current orbital elements of the actual NEA binaries in our sample (Table 1). For each binary, we search for 10 test particles closest in orbital element space to the binary's current heliocentric orbital elements using this scaling: $\delta a/a \sim \delta e \sim \delta \sin i$ (Vokrouhlický & Nesvorný 2008). Binaries 2003 YT1 and 1999 KW4 have either high inclinations and/or low semimajor axes, and these binaries proved to be difficult when searching for matches with test particles originating from the three main-source regions given by Bottke et al. (2002). In our sample of binaries, the median δa is ∼0.014 AU. The matching test particles are further integrated until they become dynamically unstable through ejection from the solar system or collision with a planet or the Sun. For each NEA binary's matching test particles, we record the orbital history with an Opik-type code similar to the procedure developed by Wetherill (1967) and implemented by Farinella & Davis (1992), which allows us to calculate the encounter velocity and intrinsic collisional probability with Earth at each time step. We calculate the intrinsic collisional probability with Earth every 10,000 years from the time of injection in the source region up to the most recent epoch at which the test particle's orbital elements matched those of the actual NEA binary. As a result, we obtain an intrinsic collisional probability value for each 10,000 year time step in the history of each matching test particle. Based on this ensemble of values we associate an average intrinsic collisional probability with each test particle by averaging all non-zero values over time. Finally, we associate an intrinsic collisional probability to each NEA binary by averaging over all of its matching test particles.

The intrinsic collisional probability (in units of km^{-2} yr^{-1}) can be multiplied by the square of an impact parameter to obtain an encounter probability (in units of yr^{-1}), whose inverse yields an approximate encounter timescale. These timescales represent the average time between encounters with Earth since injection into main belt source regions and their subsequent migration into near-Earth space.

We also calculate the close encounter timescale using an analytical, order-of-magnitude approach. Chauvineau & Farinella (1995) give the approximate timescale t

$$t \sim \frac{2\tau_{\rm coll} R_\oplus^2}{b^2} \quad (6)$$

between close encounters up to an impact parameter b given an asteroid's lifetime $\tau_{\rm coll}$ against collision with Earth of radius $R_\oplus$. For a given asteroid size, Stuart & Binzel (2004) provide the total

Table 2
Encounter Timescales (Myr) with Earth

Name	Impact parameter														
	2 $R_\oplus$	4 $R_\oplus$	6 $R_\oplus$	8 $R_\oplus$	10 $R_\oplus$	12 $R_\oplus$	14 $R_\oplus$	16 $R_\oplus$	18 $R_\oplus$	20 $R_\oplus$	22 $R_\oplus$	24 $R_\oplus$	26 $R_\oplus$	28 $R_\oplus$	30 $R_\oplus$
2000 DP107	60.73	15.18	6.75	3.80	2.43	1.69	1.24	0.95	0.75	0.61	0.50	0.42	0.36	0.31	0.27
1999 KW4	50.72	12.68	5.64	3.17	2.03	1.41	1.04	0.79	0.63	0.51	0.42	0.35	0.30	0.26	0.23
2002 CE26	391.40	97.85	43.49	24.46	15.66	10.87	7.99	6.12	4.83	3.91	3.23	2.72	2.32	2.00	1.74
2004 DC	109.90	27.47	12.21	6.87	4.40	3.05	2.24	1.72	1.36	1.10	0.91	0.76	0.65	0.56	0.49
2003 YT1	131.34	32.84	14.59	8.21	5.25	3.65	2.68	2.05	1.62	1.31	1.09	0.91	0.78	0.67	0.58
Didymos	46.30	11.58	5.14	2.89	1.85	1.29	0.94	0.72	0.57	0.46	0.38	0.32	0.27	0.24	0.21
1991 VH	72.86	18.21	8.10	4.55	2.91	2.02	1.49	1.14	0.90	0.73	0.60	0.51	0.43	0.37	0.32

Note. For each NEA binary, we show the encounter timescale (in millions of years) with Earth for various impact parameters.

number of NEAs with at least that size as well as the average interval between Earth impacts due to all asteroids of that size taken collectively. Thus, with these numbers we can calculate $\tau_{\rm coll}$ and the encounter timescale for an individual asteroid.

3.2. Results

For each binary in our sample, Table 2 gives encounter timescales with Earth from numerical simulations for impact parameters ranging from 2 $R_\oplus$ to 30 $R_\oplus$. In this impact parameter range, encounter timescales can range from $\sim 10^5$ up to $\sim 10^9$ years for the NEA binaries considered here. Encounter probabilities can be obtained by taking the inverse of these timescales, and then suitably scaled (the probability varies as the square of the impact parameter) to a desired impact parameter. Recall that due to gravitational focusing, the impact parameter b is not the same as the closest encounter distance q and are related in this manner: $b^2 = q^2(1 + (2GM_\oplus)/(q v_\infty^2))$, where G is the gravitational constant, $M_\oplus$ is the mass of Earth, and v_∞ is the encounter velocity at infinity.

Timescale estimates from the analytical approach agree with results obtained from numerical integrations within an order of magnitude for all NEA binaries in our sample. Differences in timescales can be attributed to the fact that the analytical timescales do not take into account a specific NEA's orbital trajectory as it migrates to near-Earth space, which affects its history of planetary encounters.

We repeat this analysis to determine encounter frequency with other terrestrial planets, namely, Mercury, Venus, and Mars. For a given orbital effect such as increasing a binary's eccentricity to a given value, we find that encounters with Venus are just as important as encounters with Earth. For all binaries in our sample, the encounter probabilities with Venus and Earth are comparable; these encounter probabilities for achieving a given change in the mutual orbit are a function of encounter velocity, planet mass, and binary separation.

4. DISCUSSION AND CONCLUSION

Encounter timescales presented in Table 2 show that some NEA binaries in our sample (Table 1) can typically encounter Earth frequently enough at close-enough distances to excite the binary's orbital elements, as shown by single flyby simulations in Section 2. We have presented the encounter timescales in this study, but the actual effects of encounters are also dependent on typical encounter velocities, which we plotted in Figure 1 for a generic NEA. Consideration of these factors as well as comparison to observed eccentricities are discussed in a companion paper by Fang & Margot (2012).

We briefly address the possibility of repeat encounter passes. Repeat passes, which are most relevant for binaries with short encounter timescales and large binary separations, can increase or decrease the binary's semimajor axis and eccentricity depending on its values prior to the encounter. The strength of repeat passes depends on flyby parameters such as encounter velocity. The net effect of repeat passes is still an eccentric orbit, since it is rare for an eccentric binary to undergo a planetary encounter and end up with near-zero eccentricity.

Close planetary encounters have important implications for an NEA binary's evolution, since flybys can disrupt main evolutionary processes in a binary by expanding or contracting the mutual orbit. For a typical NEA binary with a separation of $\sim$4 primary radii, we find that the semimajor axis increases on average 60% of the time for encounter distances from 2 to 10 $R_\oplus$ and encounter velocities from 8 to 24 km s^{-1}. Since flybys can increase or decrease the semimajor axis of the binary's orbit, tidal evolution can strengthen (if the semimajor axis decreases) or weaken (if the semimajor axis increases) since the tidal torque scales as the binary separation to the sixth power. When the semimajor axis is modified, the mean motion of the secondary changes and an initially spin-locked secondary may become asynchronous.[3] Asynchronization can also occur by a change in the secondary's rotation rate due to the flyby. The loss of spin-lock would imply that radiative perturbations dependent on synchronization such as BYORP would be shut down. Lastly, planetary encounters are another mechanism that may form NEA pairs. The evolution of binaries under various influences, including the planetary model presented here, is further discussed in a companion paper by Fang & Margot (2012).

To summarize, in this study we have used numerical integrations and analytical expressions to investigate the effects of planetary encounters on NEA binaries. We found the encounter distances at which flybys can increase the orbital semimajor axis, eccentricity, and inclination for a variety of encounter velocities. There is reasonable agreement between results obtained from simulations and analytical methods. The possible outcomes, including collisions, ejections, and stable encounters, are discussed for close binaries, moderately separated binaries, and

[3] In this paper, binaries with an absence of spin–orbit synchronism are called *asynchronous binaries*. Binaries with a secondary spin period synchronized to the mutual orbit period are called *synchronous binaries*. Binaries with both primary and secondary spin periods synchronized to the mutual orbit period are called *doubly synchronous binaries*. Most NEA binaries are synchronous. Note that our terminology is different from that of Pravec & Harris (2007), who used the term "asynchronous binaries" for binaries with spin–orbit synchronization. If generalization to systems with more than one satellite is needed, we affix the terms *synchronous* and *asynchronous* to the satellites being considered.

wide binaries. We have also used *N*-body integrations to examine the past evolutionary histories of NEAs as they migrated from main-belt source regions into near-Earth space. From these simulations, we calculated encounter probabilities and timescales for all NEA binaries in our sample for different impact parameters. These encounter timescales provide rough agreement with analytical estimates, which do not take into account individual NEAs' past orbital histories. Lastly, planetary encounters have important implications for evolutionary processes such as tidal and BYORP mechanisms.

We thank Bill Bottke and Ben Collins for useful discussions. We are also grateful to the reviewer for helpful comments. This work was partially supported by NASA Planetary Astronomy grant NNX09AQ68G.

REFERENCES

Asphaug, E., & Benz, W. 1996, Icarus, 121, 225
Benner, L. A. M., Margot, J. L., Nolan, M. C., et al. 2010, BAAS, 42, 1056
Binzel, R. P., Morbidelli, A., Merouane, S., et al. 2010, Nature, 463, 331
Bottke, W. F., & Melosh, H. J. 1996a, Nature, 381, 51
Bottke, W. F., Jr., & Melosh, H. J. 1996b, Icarus, 124, 372
Bottke, W. F., Morbidelli, A., Jedicke, R., et al. 2002, Icarus, 156, 399
Chambers, J. E. 1999, MNRAS, 304, 793
Chauvineau, B., & Farinella, P. 1995, Icarus, 115, 36
Collins, B. F., & Sari, R. 2008, AJ, 136, 2552
Ćuk, M. 2007, ApJ, 659, L57
Ćuk, M., & Burns, J. A. 2005, Icarus, 176, 418
Fang, J., & Margot, J. L. 2012, AJ, 143, 24
Fang, J., Margot, J., Brozovic, M., et al. 2011, AJ, 141, 154
Farinella, P. 1992, Icarus, 96, 284
Farinella, P., & Chauvineau, B. 1993, A&A, 279, 251
Farinella, P., & Davis, D. R. 1992, Icarus, 97, 111
Heggie, D. C., & Rasio, F. A. 1996, MNRAS, 282, 1064
Margot, J., Taylor, P. A., Nolan, M. C., et al. 2008, BAAS, 40, 433
Margot, J. L., Nolan, M. C., Benner, L. A. M., et al. 2002, Science, 296, 1445
Naidu, S. P., Margot, J. L., Busch, M. W., et al. 2011, in ESPC-DPS Joint Meeting, Vol. 6
Nesvorný, D., Bottke, W. F., Vokrouhlický, D., Chapman, C. R., & Rafkin, S. 2010, Icarus, 209, 510
Nolan, M. C., Howell, E. S., & Miranda, G. 2004, BAAS, 36, 1132
Ostro, S. J., Margot, J.-L., Benner, L. A. M., et al. 2006, Science, 314, 1276
Pravec, P., & Harris, A. W. 2007, Icarus, 190, 250
Pravec, P., Scheirich, P., Kušnirák, P., et al. 2006, Icarus, 181, 63
Richardson, D. C., Bottke, W. F., & Love, S. G. 1998, Icarus, 134, 47
Scheeres, D. J., Fahnestock, E. G., Ostro, S. J., et al. 2006, Science, 314, 1280
Scheeres, D. J., Marzari, F., & Rossi, A. 2004, Icarus, 170, 312
Sharma, I., Jenkins, J. T., & Burns, J. A. 2006, Icarus, 183, 312
Shepard, M. K., Margot, J.-L., Magri, C., et al. 2006, Icarus, 184, 198
Stuart, J. S., & Binzel, R. P. 2004, Icarus, 170, 295
Taylor, P. A., Margot, J. L., Nolan, M. C., et al. 2008, LPI Contributions, Vol. 1405, 8322
Vokrouhlický, D., & Nesvorný, D. 2008, AJ, 136, 280
Walsh, K. J., & Richardson, D. C. 2006, Icarus, 180, 201
Wetherill, G. W. 1967, J. Geophys. Res., 72, 2429